JOURNAL OF GUIDANCE, CONTROL, AND DYNAMICS
Vol. 18, No. 5, September–October 1995

Engineering Notes

ENGINEERING NOTES are short manuscripts describing new developments or important results of a preliminary nature. These Notes cannot exceed 6 manuscript pages and 3 figures; a page of text may be substituted for a figure and vice versa. After informal review by the editors, they may be published within a few months of the date of receipt. Style requirements are the same as for regular contributions (see inside back cover).

Distributed Control of Maneuvering Vehicles for On-Orbit Assembly

Colin R. McInnes*
University of Glasgow,
Glasgow G12 8QQ, Scotland, United Kingdom

Nomenclature

G	= set, defines connection between nodes of ith and jth components
G', G''	= subsets of G
κ_i, $\tilde{\kappa}_i$	= positive constants
ϕ_i	= local gravitational potential experienced by ith component
Ω	= angular velocity of frame T' on reference orbit

Introduction

ON-ORBIT assembly of space structures has long been considered as a means of enabling the construction of large space platforms. Many scenarios envisage robotic maneuvering vehicles in the assembly process as the primary means of construction.[1] In this Note an analytical method is developed that allows robotic assembly of components through the emergent properties of the dynamics of the system. Treating the ensemble of robotic maneuvering vehicles and components as the global system, a naturally distributed control is generated that guarantees assembly of the components of the system. Control forces and moments are provided in analytic form that represent the controls required for each of the maneuvering vehicles to ensure assembly of the system of components. The method discussed is seen as a possible means of allowing simple assembly tasks to be achieved without using complex artificial intelligence schemes to drive the assembly process. Although the current study uses rather artificial dynamics and assumptions, it demonstrates that complex assembly tasks can be carried out using simple rules.

System Dynamics

In this section the dynamics of the system are developed and equations of relative motion derived. The system dynamics will be considered in an orbiting frame T' relative to an inertial frame T (Fig. 1). The orbiting frame is assumed to represent a circular orbit at position $\boldsymbol{R}_s$ relative to the inertial frame. The components of the assembly will be treated as uniform beams with a known inertia tensor $\boldsymbol{I}_i$ and mass m_i ($i = 1, \ldots, N$), where N is the total number of components. Similarly, the maneuvering vehicle S_i that translates and rotates the ith component will be considered as a point mass $\tilde{m}_i$. Each component will be described by vectors $\boldsymbol{r}_i$ and $\tilde{\boldsymbol{r}}_i$ defining the location of its endpoints, a vector $\boldsymbol{L}_i$ describing its length and orientation, and a vector $\boldsymbol{\rho}_i$ defining its center of mass. The ith component is maneuvered by a vehicle S_i that then generates a center-of-mass force $\boldsymbol{f}_i$ and torque $\boldsymbol{\Gamma}_i$.

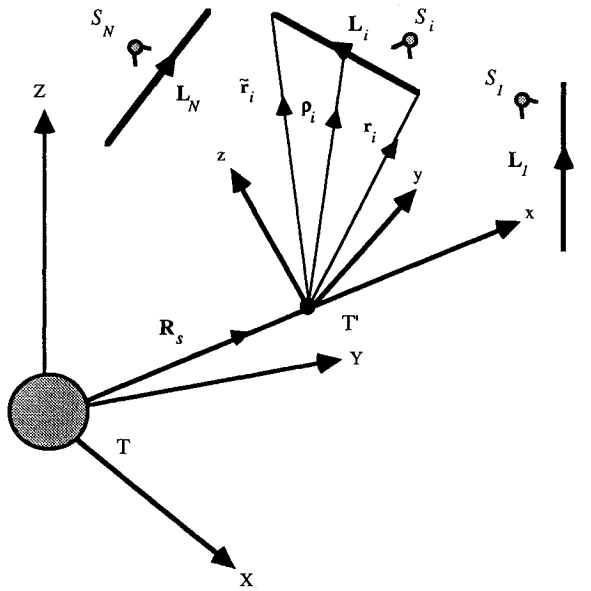

Fig. 1 Schematic geometry of components relative to orbiting frame T'.

The inertial location of the center of mass of the ith component $\boldsymbol{R}_i$ is given by $\boldsymbol{R}_s + \boldsymbol{\rho}_i$ so that its equation of motion may be written in the rotating frame T' as

$$\frac{\mathrm{d}^2\boldsymbol{R}_i}{\mathrm{d}t^2} + 2\Omega \times \frac{\mathrm{d}\boldsymbol{R}_i}{\mathrm{d}t} + \Omega \times (\Omega \times \boldsymbol{R}_i) = \frac{1}{m_i + \tilde{m}_i}\boldsymbol{f}_i - \nabla\phi_i \quad (1)$$

In the subsequent analysis the assembly times will be significantly shorter than one orbital period and the control forces and torques will be significantly larger than the difference between the gravitational and rotating frame forces represented in Eq. (1). These forces will be ignored so that the equations of motion of the ith component will be given by

$$\frac{\mathrm{d}^2\boldsymbol{\rho}_i}{\mathrm{d}t^2} = \frac{1}{m_i + \tilde{m}_i}\boldsymbol{f}_i \quad (2a)$$

$$\boldsymbol{I}_i \cdot \dot{\omega}_i + \omega_i \times (\boldsymbol{I}_i \cdot \omega_i) = \boldsymbol{\Gamma}_i \quad (2b)$$

The additional forces in Eq. (1) may be added to the required control force if necessary. These equations of motion may now be used to develop the required distributed control.

Distributed Control

To assemble the components, Lyapunov's theorem will be used along with a scalar artificial potential function. The potential function method has been developed for other spacecraft control applications.[2–4] In order to assemble the system, each component will experience an acceleration due to the potential of the node to which it is to connect. Then over a period of time, the assembled structure will emerge as an asymptotic solution of the dynamics of the system. In this initial study the components are allowed to cross, inducing contact forces. However, by making each component a line source of potential, such contacts may be avoided.

Received Feb. 1, 1995; revision received April 11, 1995; accepted for publication May 1, 1995.

*Lecturer, Department of Aerospace Engineering.

The potential function V may be written in arbitrary form as

$$V = \frac{1}{2}\sum_{\substack{i=1\\ i,j\in G}}^{N}\sum_{j=1}^{N}\lambda_{ij} f\left[(\tilde{r}_i - r_j)^2\right] + \frac{1}{2}\sum_{i=1}^{N}(v_i \cdot v_i + \omega_i \cdot \omega_i) \quad (3)$$

Clearly this function is zero when the correct nodes have been connected and the rotational and translational velocities are zero. The constants λ_{ij} are chosen such that V is positive definite and may be used to shape the behavior of the assembly sequence, as can the function f. The time rate of change of the potential is found to be

$$\dot{V} = \sum_{\substack{i=1\\ i,j\in G}}^{N}\sum_{j=1}^{N}\lambda_{ij}\nabla f\left[(\tilde{r}_i - r_j)^2\right](\tilde{v}_i - v_j) + \sum_{i=1}^{N}(v_i \cdot \dot{v}_i + \omega_i \cdot \dot{\omega}_i) \quad (4)$$

However, the velocity $\tilde{v}_i$ of the endpoint $\tilde{r}_i$ may be written in terms of the velocity v_i of the opposite endpoint r_i using

$$\tilde{v}_i = v_i + \omega_i \times L_i \quad (5)$$

This relation also enforces the constraint that the length of each element is constant. Therefore, using the vector triple-product identity

$$\nabla f \cdot (\omega_i \times L_i) = -\omega_i \cdot (\nabla f \times L_i) \quad (6)$$

the rate of change of the potential function may be written as

$$\dot{V} = \sum_{i=1}^{N} v_i \cdot \left(\dot{v}_i + \sum_{\substack{l=1\\ l,m\in G'}}^{N}\sum_{m=1}^{N}\lambda_{lm}\nabla f\right) + \sum_{i=1}^{N}\omega_i \cdot \left[\dot{\omega}_i + \left(\sum_{\substack{p=1\\ p,q\in G''}}^{N}\sum_{q=1}^{N}\lambda_{pq}\nabla f\right) \times L_i\right] \quad (7)$$

In order to ensure that the rate of descent of the potential is negative definite, the following translational and rotational accelerations will be chosen:

$$\dot{v}_i = -\kappa_i v_i - \sum_{\substack{l=1\\ l,m\in G'}}^{N}\sum_{m=1}^{N}\lambda_{lm}\nabla f \quad (8a)$$

$$\dot{\omega}_i = -\tilde{\kappa}_i \omega_i - \left(\sum_{\substack{p=1\\ l,m\in G'}}^{N}\sum_{q=1}^{N}\lambda_{pq}\nabla f\right) \times L_i \quad (8b)$$

The rate of descent of the potential is then given by

$$\dot{V} = -\sum_{i=1}^{N}\kappa_i v_i \cdot v_i - \sum_{i=1}^{N}\tilde{\kappa}_i \omega_i \cdot \omega_i \quad (9)$$

which is clearly negative definite. As $V \to 0$, the components will then be assembled into the desired configuration with zero rotational and translational velocities.

The endpoint acceleration $\dot{v}_i$ may be written as a center-of-mass acceleration $\dot{v}_i^c$ by the transformation

$$\dot{v}_i^c = \dot{v}_i - \tfrac{1}{2}\omega_i \times (\omega \times L_i) - \tfrac{1}{2}\dot{\omega}_i \times L_i \quad (10)$$

which includes the centripetal and angular accelerations of the ith component due to its rotational motion about its center of mass. Therefore, using Eqs. (2) the required center-of-mass force and torque required to control the assembly may be obtained.

Triangular Truss Assembly

In this section an example of a simple assembly problem will be considered. Three equal beams will be assembled into a triangular truss section using an equal number of maneuvering vehicles. The potential of the system will therefore be written as

$$V = \frac{1}{2}\lambda\left[(\tilde{r}_1 - r_2)^2 + (\tilde{r}_2 - r_3)^2 + (\tilde{r}_3 - r_1)^2\right] + \frac{1}{2}\sum_{i=1}^{3} v_i \cdot v_i + \omega_i \cdot \omega_i \quad (11)$$

where the initial location of these nodes is illustrated in Fig. 2. Using the method described in the previous section, expressions for the required endpoint translational accelerations may then be derived as

$$\dot{v}_1 = -\kappa v_1 - \lambda[(\tilde{r}_1 - r_2) - (\tilde{r}_3 - r_1)] \quad (12a)$$

$$\dot{v}_2 = -\kappa v_2 - \lambda[(\tilde{r}_2 - r_3) - (\tilde{r}_1 - r_2)] \quad (12b)$$

$$\dot{v}_3 = -\kappa v_3 - \lambda[(\tilde{r}_3 - r_1) - (\tilde{r}_2 - r_3)] \quad (12c)$$

where κ and λ are constant shaping parameters. These controls may then be transformed to the required center-of-mass accelerations using Eq. (10). The required angular accelerations may also be derived as

$$\dot{\omega}_1 = -\tilde{\kappa}\omega_1 - \lambda(\tilde{r}_1 - r_2) \times L_1 \quad (13a)$$

$$\dot{\omega}_2 = -\tilde{\kappa}\omega_2 - \lambda(\tilde{r}_2 - r_3) \times L_2 \quad (13b)$$

$$\dot{\omega}_3 = -\tilde{\kappa}\omega_3 - \lambda(\tilde{r}_3 - r_1) \times L_3 \quad (13c)$$

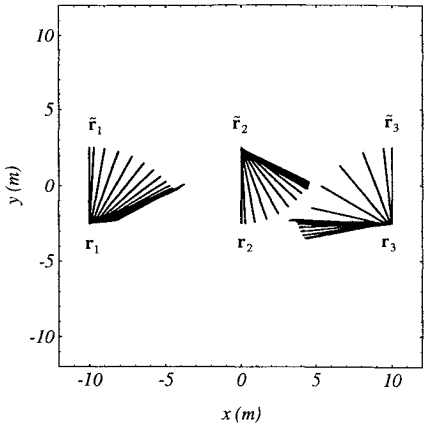

a) t = 0–10 s

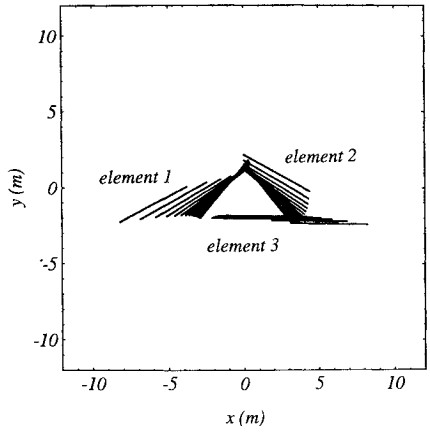

b) t = 10–180 s

Fig. 2 Assembly of three components into triangular truss.

Using these controls the rate of descent of the potential of the system is seen to be negative definite:

$$\dot{V} = -\kappa \sum_{i=1}^{3} v_i \cdot v_i - \tilde{\kappa} \sum_{i=1}^{3} \omega_i \cdot \omega_i \qquad (14)$$

so that the triangular truss section will be assembled from an initial configuration of the three beam elements. A planar assembly sequence is shown in Fig. 2 with $\lambda = 0.01$, $\kappa = 5$, and $\tilde{\kappa} = 5$. It can be seen that components are rotated and translated such that the desired triangular configuration is formed. The constants can be used to shape the maneuver and to control the maximum required translational forces and rotational torques.

Conclusions

A naturally distributed control has been developed that provides translational accelerations and rotational torques in analytical form for multiple-maneuvering vehicles assembling connected components of a space structure. The development is based upon Lyapunov's method, which ensures that the assembly is constructed from the initial configuration of components. Since the control accelerations and torques are provided in analytic form, complex algorithms are not required to assemble the components.

References

[1]Waltz, D. M., *On-Orbit Servicing of Space Systems*, Krieger, FL, 1993.

[2]McInnes, C. R., "Large Angle Slew Maneuvers with Autonomous Sun Vector Avoidance," *Journal of Guidance, Control, and Dynamics*, Vol. 17, No. 4, 1991, pp. 875–877.

[3]McInnes, C. R., "Autonomous Ring Formation for a Constellation of Satellites," Dept. of Aerospace Engineering, Univ. of Glasgow, Rept. 9426, Glasgow, Scotland, UK, 1994.

[4]McInnes, C. R., "Autonomous Proximity Maneuvering Using Artificial Potential Functions," *ESA Journal*, Vol. 17, 1993, pp. 159–169.

Optimal Direct Ascent with Carrier Return to Base

G. Sachs* and R. Bayer†
Technische Universität München, Munich 80290, Germany

Introduction

THERE is currently a great interest in new concepts for advanced space transportation systems. A promising concept is a two-stage system comprising a lifting carrier vehicle equipped with a turbo-/ramjet combination and a lifting orbital stage propelled by a rocket.

Ascent optimization of advanced two-stage flight systems for minimizing fuel is subject of recent research.[1–7] Results for ascents basically show an acceleration/climb trajectory to reach a separation flight condition that is favorable for releasing the orbital stage, which then performs an ascent to an orbit. After separation, the carrier vehicle returns to its base for landing. When no range requirement for the destination of separation exists, a direct ascent is performed, the first part of which is usually considered as a noncurved trajectory in a vertical plane until separation.[3–7] Only after the separation is finished, the trajectory of the carrier shows a turn for heading back to the base.

Received March 25, 1994; revision received Feb. 1, 1995; accepted for publication March 18, 1995.

*Prof. Dr.-Ing., Director, Institute of Flight Mechanics and Flight Control. Associate Fellow AIAA.

†Dr.-Ing., Scientist, Institute of Flight Mechanics and Flight Control. Member AIAA.

It is the purpose of this Note to show that this type of ascent trajectory is not generally fuel minimal. Rather, it will be shown that the optimal solution can be a highly curved trajectory from the very beginning. Thus, there is a pronounced motion in three dimensions already before separation.

Optimal Curved Ascent Trajectory

Optimization results for fuel minimization are presented in Fig. 1, which shows ground tracks of two direct ascent trajectories with return of the carrier vehicle to the base. An uncurved trajectory is shown as a reference that is usually considered as the optimal solution type (dashed line). However, the optimal solution is a highly curved trajectory from the very beginning (nondashed line). The optimal curved trajectory depicted in Fig. 1 shows a heading change of about 210 deg before separation takes place. After separation, both trajectories have a similar structure as regards a turn for heading back to the base. However, the distance between separation location and base is significantly smaller for the optimal solution than for the reference trajectory.

Further details are presented in Figs. 2 and 3, which show state and control variables histories (with equivalence ratio ϕ_f as a measure of thrust). The primary difference during the first flight phase,

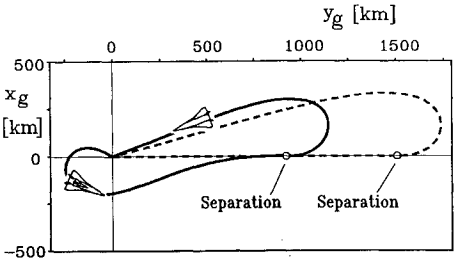

Fig. 1 Ascent trajectories with carrier return to base: —, optimal curved ascent trajectory, m_f = 63.9 mg; and - - - -, vertical plane ascent trajectory, m_f = 64.7 mg.

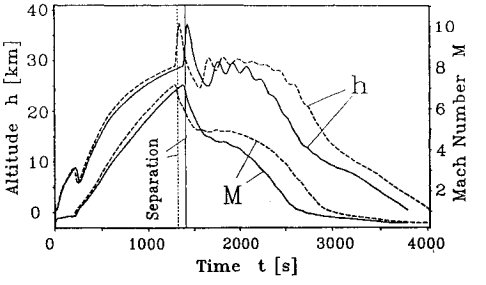

Fig. 2 State variables of ascent trajectories with carrier return to base: —, optimal curved ascent trajectory, m_f = 63.9 mg; and - - - -, vertical plane ascent trajectory, m_f = 64.7 mg.

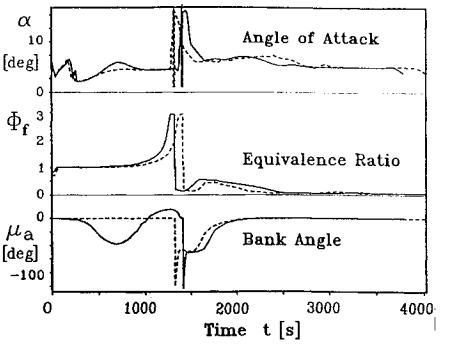

Fig. 3 Control variables of ascent trajectories with carrier return to base: —, optimal curved ascent trajectory, m_f = 63.9 mg; and - - - -, vertical plane ascent trajectory, m_f = 64.7 mg.